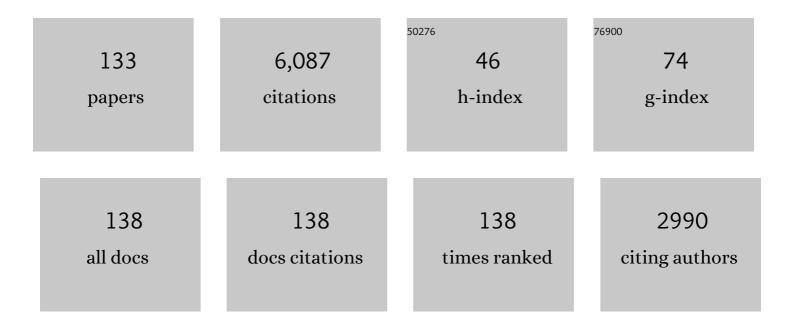
## List of Publications by Year in descending order

Source: https://exaly.com/author-pdf/2684683/publications.pdf Version: 2024-02-01



I RVAN RVCC

#	Article	IF	CITATIONS
1	Measuring the melting curve of iron at super-Earth core conditions. Science, 2022, 375, 202-205.	12.6	39
2	Species separation in polystyrene shock release evidenced by molecular-dynamics simulations and laser-drive experiments. Physical Review Research, 2022, 4, .	3.6	0
3	Diamond formation in double-shocked epoxy to 150 CPa. Journal of Applied Physics, 2022, 131, .	2.5	6
4	Structure and density of silicon carbide to 1.5 TPa and implications for extrasolar planets. Nature Communications, 2022, 13, 2260.	12.8	11
5	Structural complexity in ramp-compressed sodium to 480 GPa. Nature Communications, 2022, 13, 2534.	12.8	14
6	Emission phases of implosion sources for x-ray absorption fine structure spectroscopy. Physics of Plasmas, 2022, 29, .	1.9	5
7	Planar, longitudinal, compressive waves in solids: Thermodynamics and uniaxial strain restrictions. Journal of Applied Physics, 2022, 131, 215904.	2.5	1
8	Evidence for Dissociation and Ionization in Shock Compressed Nitrogen to 800ÂGPa. Physical Review Letters, 2022, 129, .	7.8	7
9	A case study of using x-ray Thomson scattering to diagnose the in-flight plasma conditions of DT cryogenic implosions. Physics of Plasmas, 2022, 29, 072703.	1.9	7
10	Metastability of diamond ramp-compressed to 2 terapascals. Nature, 2021, 589, 532-535.	27.8	79
11	Implications of the iron oxide phase transition on the interiors of rocky exoplanets. Nature Geoscience, 2021, 14, 121-126.	12.9	28
12	Equation-of-state, sound speed, and reshock of shock-compressed fluid carbon dioxide. Physics of Plasmas, 2021, 28, .	1.9	5
13	Shock-compressed silicon: Hugoniot and sound speed up to 2100 GPa. Physical Review B, 2021, 103, .	3.2	13
14	High-energy-density-physics measurements in implosions using Bayesian inference. Physics of Plasmas, 2021, 28, .	1.9	8
15	Evidence of hydrogenâ~'helium immiscibility at Jupiter-interior conditions. Nature, 2021, 593, 517-521.	27.8	41
16	Polymorphism of gold under laser-based ramp compression to 690 GPa. Physical Review B, 2021, 103, .	3.2	11
17	Melting of Tantalum at Multimegabar Pressures on the Nanosecond Timescale. Physical Review Letters, 2021, 126, 255701.	7.8	11
18	Melting of magnesium oxide up to two terapascals using double-shock compression. Physical Review B, 2021, 104, .	3.2	11

#	Article	IF	CITATIONS
19	Density evolution after shock release from laser-driven polystyrene (CH) targets in inertial confinement fusion. Physics of Plasmas, 2021, 28, .	1.9	2
20	Improved first-principles equation-of-state table of deuterium for high-energy-density applications. Physical Review B, 2021, 104, .	3.2	8
21	Equation of State of <mml:math <br="" xmlns:mml="http://www.w3.org/1998/Math/MathML">display="inline"&gt;<mml:mrow><mml:msub><mml:mrow><mml:mi>CO</mml:mi></mml:mrow><ml:mrow><m Shock Compressed to 1ÂTPa. Physical Review Letters, 2020, 125, 165701.</m </ml:mrow></mml:msub></mml:mrow></mml:math>	ml <b>:me</b> >2<	/m <b>nb&amp;</b> mn>
22	Energy Flow in Thin Shell Implosions and Explosions. Physical Review Letters, 2020, 125, 215001.	7.8	8
23	Saturn-ring proton backlighters for the National Ignition Facility. Review of Scientific Instruments, 2020, 91, 093505.	1.3	2
24	Constraining physical models at gigabar pressures. Physical Review E, 2020, 102, 053210.	2.1	11
25	Localized mix-induced radiative cooling in a capsule implosion at the National Ignition Facility. Physical Review E, 2020, 101, 033205.	2.1	25
26	X-ray diffraction at the National Ignition Facility. Review of Scientific Instruments, 2020, 91, 043902.	1.3	42
27	Experimental study of energy transfer in double shell implosions. Physics of Plasmas, 2019, 26, .	1.9	32
28	Nanosecond X-ray diffraction of shock-compressed superionic water ice. Nature, 2019, 569, 251-255.	27.8	215
29	Response to Comment on "Insulator-metal transition in dense fluid deuterium― Science, 2019, 363, .	12.6	5
30	Breakdown of Fermi Degeneracy in the Simplest Liquid Metal. Physical Review Letters, 2019, 122, 085001.	7.8	6
31	Optimized x-ray sources for x-ray diffraction measurements at the Omega Laser Facility. Review of Scientific Instruments, 2019, 90, 125113.	1.3	25
32	A boundary condition for Guderley's converging shock problem. Physics of Fluids, 2019, 31, .	4.0	12
33	Measuring the shock impedance mismatch between high-density carbon and deuterium at the National Ignition Facility. Physical Review B, 2018, 97, .	3.2	21
34	Crystal structure and equation of state of Fe-Si alloys at super-Earth core conditions. Science Advances, 2018, 4, eaao5864.	10.3	56
35	Experimental evidence for superionic water ice using shock compression. Nature Physics, 2018, 14, 297-302.	16.7	165
36	First demonstration of improved capsule implosions by reducing radiation preheat in uranium vs gold hohlraums. Physics of Plasmas, 2018, 25, .	1.9	17

#	Article	IF	CITATIONS
37	Using a 2-shock 1D platform at NIF to measure the effect of convergence on mix and symmetry. Physics of Plasmas, 2018, 25, 102702.	1.9	6
38	Implosion shape control of high-velocity, large case-to-capsule ratio beryllium ablators at the National Ignition Facility. Physics of Plasmas, 2018, 25, 072708.	1.9	16
39	Conceptual design for time-resolved x-ray diffraction in a single laser-driven compression experiment. AIP Conference Proceedings, 2018, , .	0.4	4
40	X-ray diffraction of ramp-compressed aluminum to 475 GPa. Physics of Plasmas, 2018, 25, .	1.9	17
41	Insulator-metal transition in dense fluid deuterium. Science, 2018, 361, 677-682.	12.6	108
42	Examining the radiation drive asymmetries present in the high foot series of implosion experiments at the National Ignition Facility. Physics of Plasmas, 2017, 24, .	1.9	31
43	The role of hot spot mix in the low-foot and high-foot implosions on the NIF. Physics of Plasmas, 2017, 24, .	1.9	49
44	Symmetry control of an indirectly driven high-density-carbon implosion at high convergence and high velocity. Physics of Plasmas, 2017, 24, .	1.9	106
45	Measurement of Body-Centered-Cubic Aluminum at 475ÂGPa. Physical Review Letters, 2017, 119, 175702.	7.8	37
46	Performance of beryllium targets with full-scale capsules in low-fill 6.72-mm hohlraums on the National Ignition Facility. Physics of Plasmas, 2017, 24, .	1.9	14
47	Hugoniot and release measurements in diamond shocked up to 26 Mbar. Physical Review B, 2017, 95, .	3.2	32
48	Use of 41Ar production to measure ablator areal density in NIF beryllium implosions. Physics of Plasmas, 2017, 24, .	1.9	2
49	A novel method to recover DD fusion proton CR-39 data corrupted by fast ablator ions at OMEGA and the National Ignition Facility. Review of Scientific Instruments, 2016, 87, 11D812.	1.3	2
50	Control of Be capsule low mode implosions symmetry at the National Ignition Facility. Journal of Physics: Conference Series, 2016, 717, 012033.	0.4	2
51	NIF Rugby High Foot Campaign from the design side. Journal of Physics: Conference Series, 2016, 717, 012035.	0.4	4
52	Development of a WDM platform for charged-particle stopping experiments. Journal of Physics: Conference Series, 2016, 717, 012118.	0.4	4
53	Capsule Ablator Inflight Performance Measurements Via Streaked Radiography Of ICF Implosions On The NIF*. Journal of Physics: Conference Series, 2016, 688, 012014.	0.4	9
54	X-ray scattering measurements of dissociation-induced metallization of dynamically compressed deuterium. Nature Communications, 2016, 7, 11189.	12.8	27

#	Article	IF	CITATIONS
55	First beryllium capsule implosions on the National Ignition Facility. Physics of Plasmas, 2016, 23, 056310.	1.9	37
56	Resolving hot spot microstructure using x-ray penumbral imaging (invited). Review of Scientific Instruments, 2016, 87, 11E201.	1.3	38
57	The near vacuum hohlraum campaign at the NIF: A new approach. Physics of Plasmas, 2016, 23, .	1.9	51
58	Effects of fuel-capsule shimming and drive asymmetry on inertial-confinement-fusion symmetry and yield. Physics of Plasmas, 2016, 23, .	1.9	17
59	Experimental room temperature hohlraum performance study on the National Ignition Facility. Physics of Plasmas, 2016, 23, .	1.9	6
60	X-ray diffraction of molybdenum under ramp compression to 1 TPa. Physical Review B, 2016, 94, .	3.2	33
61	Development of Improved Radiation Drive Environment for High Foot Implosions at the National Ignition Facility. Physical Review Letters, 2016, 117, 225002.	7.8	61
62	X-ray drive of beryllium capsule implosions at the National Ignition Facility. Journal of Physics: Conference Series, 2016, 717, 012058.	0.4	3
63	Symmetry tuning of a near one-dimensional 2-shock platform for code validation at the National Ignition Facility. Physics of Plasmas, 2016, 23, .	1.9	33
64	X-ray diffraction of molybdenum under shock compression to 450 GPa. Physical Review B, 2015, 92, .	3.2	38
65	X-Ray Diffraction of Solid Tin to 1.2ÂTPa. Physical Review Letters, 2015, 115, 075502.	7.8	52
66	Analysis of laser shock experiments on precompressed samples using a quartz reference and application to warm dense hydrogen and helium. Journal of Applied Physics, 2015, 118, .	2.5	69
67	Note: A monoenergetic proton backlighter for the National Ignition Facility. Review of Scientific Instruments, 2015, 86, 116104.	1.3	23
68	Overview of Performance and Progress with Inertially Confined Fusion Implosions on the National Ignition Facility. , 2015, , .		0
69	2015, 22, 056314.	1.9	49
70	First High-Convergence Cryogenic Implosion in a Near-Vacuum Hohlraum. Physical Review Letters, 2015, 114, 175001.	7.8	117
71	Cryogenic tritium-hydrogen-deuterium and deuterium-tritium layer implosions with high density carbon ablators in near-vacuum hohlraums. Physics of Plasmas, 2015, 22, 062703.	1.9	62
72		1.9	82

#	Article	IF	CITATIONS
73	Measurement of Charged-Particle Stopping in Warm Dense Plasma. Physical Review Letters, 2015, 114, 215002.	7.8	107
74	Thin Shell, High Velocity Inertial Confinement Fusion Implosions on the National Ignition Facility. Physical Review Letters, 2015, 114, 145004.	7.8	56
75	of Plasmas, 2015, 22, 056318.	1.9	80
76	Effect of the mounting membrane on shape in inertial confinement fusion implosions. Physics of Plasmas, 2015, 22, .	1.9	85
77	In-flight observations of low-mode <i>ï</i> R asymmetries in NIF implosions. Physics of Plasmas, 2015, 22,	1.9	24
78	Investigation of ion kinetic effects in direct-drive exploding-pusher implosions at the NIF. Physics of Plasmas, 2014, 21, 122712.	1.9	33
79	The effect of shock dynamics on compressibility of ignition-scale National Ignition Facility implosions. Physics of Plasmas, 2014, 21, .	1.9	20
80	A magnetic particle time-of-flight (MagPTOF) diagnostic for measurements of shock- and compression-bang time at the NIF (invited). Review of Scientific Instruments, 2014, 85, 11D901.	1.3	12
81	Reconstruction of 2D x-ray radiographs at the National Ignition Facility using pinhole tomography (invited). Review of Scientific Instruments, 2014, 85, 11E503.	1.3	13
82	Kinetic mix mechanisms in shock-driven inertial confinement fusion implosions. Physics of Plasmas, 2014, 21, .	1.9	15
83	2D X-Ray Radiography of Imploding Capsules at the National Ignition Facility. Physical Review Letters, 2014, 112, 195001.	7.8	154
84	Dynamic symmetry of indirectly driven inertial confinement fusion capsules on the National Ignition Facility. Physics of Plasmas, 2014, 21, .	1.9	81
85	X-ray area backlighter development at the National Ignition Facility (invited). Review of Scientific Instruments, 2014, 85, 11D502.	1.3	22
86	High-density carbon ablator experiments on the National Ignition Facility. Physics of Plasmas, 2014, 21, .	1.9	116
87	The high-foot implosion campaign on the National Ignition Facility. Physics of Plasmas, 2014, 21, .	1.9	149
88	Reduced instability growth with high-adiabat high-foot implosions at the National Ignition Facility. Physical Review E, 2014, 90, 011102.	2.1	77
89	Solid Iron Compressed Up to 560 GPa. Physical Review Letters, 2013, 111, 065501.	7.8	137
90	T–T Neutron Spectrum from Inertial Confinement Implosions. Few-Body Systems, 2013, 54, 1599-1602.	1.5	0

#	Article	IF	CITATIONS
91	Diagnosing implosion performance at the National Ignition Facility (NIF) by means of neutron spectrometry. Nuclear Fusion, 2013, 53, 043014.	3.5	84
92	Experimental evidence for a phase transition in magnesium oxide at exoplanet pressures. Nature Geoscience, 2013, 6, 926-929.	12.9	170
93	Observation of strong electromagnetic fields around laser-entrance holes of ignition-scale hohlraums in inertial-confinement fusion experiments at the National Ignition Facility. New Journal of Physics, 2013, 15, 025040.	2.9	14
94	The magnetic recoil spectrometer for measurements of the absolute neutron spectrum at OMEGA and the NIF. Review of Scientific Instruments, 2013, 84, 043506.	1.3	59
95	Progress toward ignition at the National Ignition Facility. Plasma Physics and Controlled Fusion, 2013, 55, 124015.	2.1	23
96	Time evolution of filamentation and self-generated fields in the coronae of directly driven inertial-confinement fusion capsules. Physics of Plasmas, 2012, 19, .	1.9	38
97	Charged-particle spectroscopy for diagnosing shock ÏR and strength in NIF implosions. Review of Scientific Instruments, 2012, 83, 10D901.	1.3	38
98	A novel particle time of flight diagnostic for measurements of shock- and compression-bang times in D3He and DT implosions at the NIF. Review of Scientific Instruments, 2012, 83, 10D902.	1.3	38
99	display="inline"> <mml:mi mathvariant="bold">T</mml:mi> <mml:mo stretchy="false"&gt;(<mml:mi>t</mml:mi><mml:mo>,</mml:mo><mml:mn>2</mml:mn><mml:mi>n&lt; /&gt;<mml:none></mml:none><mml:mn>4</mml:mn>Neutron Spectrum at Low</mml:mi></mml:mo 	<	mml;mo) Tj E
100	Reactant Energies from Inertial Confinement Implosions, Physical Review Letters, 2012, 109, 025003. Powder diffraction from solids in the terapascal regime. Review of Scientific Instruments, 2012, 83, 113904.	1.3	84
101	Implosion dynamics measurements at the National Ignition Facility. Physics of Plasmas, 2012, 19, .	1.9	125
102	Neutron spectrometry—An essential tool for diagnosing implosions at the National Ignition Facility (invited). Review of Scientific Instruments, 2012, 83, 10D308.	1.3	117
103	Extended data set for the equation of state of warm dense hydrogen isotopes. Physical Review B, 2012, 86, .	3.2	95
104	Evidence for Stratification of Deuterium-Tritium Fuel in Inertial Confinement Fusion Implosions. Physical Review Letters, 2012, 108, 075002.	7.8	61
105	Compressing magnetic fields with high-energy lasers. Physics of Plasmas, 2010, 17, .	1.9	89
106	An imaging proton spectrometer for short-pulse laser plasma experiments. Review of Scientific Instruments, 2010, 81, 10D314.	1.3	14
107	Laser-Driven Magnetic-Flux Compression in High-Energy-Density Plasmas. Physical Review Letters, 2009, 103, 215004.	7.8	91
108	Lorentz Mapping of Magnetic Fields in Hot Dense Plasmas. Physical Review Letters, 2009, 103, 085001.	7.8	43

#	Article	IF	CITATIONS
109	Electron-ion thermal equilibration after spherical shock collapse. Physical Review E, 2009, 80, 026403.	2.1	15
110	Observations of Electromagnetic Fields and Plasma Flow in Hohlraums with Proton Radiography. Physical Review Letters, 2009, 102, 205001.	7.8	69
111	Proton radiography of dynamic electric and magnetic fields in laser-produced high-energy-density plasmas. Physics of Plasmas, 2009, 16, .	1.9	31
112	Diagnosing ablator ÏR and ÏR asymmetries in capsule implosions using charged-particle spectrometry at the National Ignition Facility. Physics of Plasmas, 2009, 16, 022702.	1.9	10
113	Study of direct-drive capsule implosions in inertial confinement fusion with proton radiography. Plasma Physics and Controlled Fusion, 2009, 51, 014003.	2.1	5
114	Proton Radiography of Inertial Fusion Implosions. Science, 2008, 319, 1223-1225.	12.6	157
115	Monoenergetic-Proton-Radiography Measurements of Implosion Dynamics in Direct-Drive Inertial-Confinement Fusion. Physical Review Letters, 2008, 100, 225001.	7.8	85
116	Observations of the collapse of asymmetrically driven convergent shocks. Physics of Plasmas, 2008, 15, .	1.9	23
117	An accelerator based fusion-product source for development of inertial confinement fusion nuclear diagnostics. Review of Scientific Instruments, 2008, 79, 043302.	1.3	9
118	First measurements of the absolute neutron spectrum using the magnetic recoil spectrometer at OMEGA (invited). Review of Scientific Instruments, 2008, 79, 10E502.	1.3	78
119	Nuclear measurements of fuel-shell mix in inertial confinement fusion implosions at OMEGA. Physics of Plasmas, 2007, 14, 056306.	1.9	14
120	Observation of the Decay Dynamics and Instabilities of Megagauss Field Structures in Laser-Produced Plasmas. Physical Review Letters, 2007, 99, 015001.	7.8	48
121	Observation of Megagauss-Field Topology Changes due to Magnetic Reconnection in Laser-Produced Plasmas. Physical Review Letters, 2007, 99, 055001.	7.8	151
122	Time-Dependent Nuclear Measurements of Mix in Inertial Confinement Fusion. Physical Review Letters, 2007, 98, 215002.	7.8	24
123	Monoenergetic proton backlighter for measuring E and B fields and for radiographing implosions and high-energy density plasmas (invited). Review of Scientific Instruments, 2006, 77, 10E725.	1.3	58
124	Measured dependence of nuclear burn region size on implosion parameters in inertial confinement fusion experiments. Physics of Plasmas, 2006, 13, 082704.	1.9	14
125	Tests of the hydrodynamic equivalence of direct-drive implosions with different D2 and He3 mixtures. Physics of Plasmas, 2006, 13, 052702.	1.9	60
126	Proton core imaging of the nuclear burn in inertial confinement fusion implosions. Review of Scientific Instruments, 2006, 77, 043503.	1.3	17

#	Article	IF	CITATIONS
127	MeasuringEandBFields in Laser-Produced Plasmas with Monoenergetic Proton Radiography. Physical Review Letters, 2006, 97, 135003.	7.8	192
128	Using nuclear data and Monte Carlo techniques to study areal density and mix in D2 implosions. Physics of Plasmas, 2005, 12, 032703.	1.9	18
129	Measuring shock-bang timing and ÏR evolution of D3He implosions at OMEGA. Physics of Plasmas, 2004, 11, 2798-2805.	1.9	41
130	D3He-proton emission imaging for inertial-confinement-fusion experiments (invited). Review of Scientific Instruments, 2004, 75, 3520-3525.	1.3	46
131	Spectrometry of charged particles from inertial-confinement-fusion plasmas. Review of Scientific Instruments, 2003, 74, 975-995.	1.3	214
132	Measuring Implosion Dynamics throughÏ <b>R</b> Evolution in Inertial-Confinement Fusion Experiments. Physical Review Letters, 2003, 90, 095002.	7.8	39
133	Capsule-areal-density asymmetries inferred from 14.7-MeV deuterium–helium protons in direct-drive OMEGA implosions. Physics of Plasmas, 2003, 10, 1919-1924.	1.9	13